European Review for Medical and Pharmacological Sciences 2020; 24: 9633-9644

Knockdown of NEAT1 mitigates ox-LDL-induced injury in human umbilical vein endothelial cells *via* miR-30c-5p/TCF7 axis

J.-T. GUO, L. WANG, H.-B. YU

Department of Cardiac Surgery, The First Hospital of Jilin University, Jilin, China

Abstract. – OBJECTIVE: Atherosclerosis is an inflammation-associated disease resulting in a huge health hazard. Abundance of researches showed that long non-coding RNAs (lncRNAs) played vital roles in atherosclerosis, but the molecular mechanism of nuclear-enriched abundant transcript (NEAT1) has not been fully elucidated yet.

PATIENTS AND METHODS: Human umbilical vein endothelial cells (HUVECs) were treated with oxidized low-density lipoprotein (ox-LDL) for constructing the model of atherosclerosis. The detection of NEAT1, microRNA-30c-5p (miR-30c-5p), and transcription factor 7 (TCF7) expression was implemented by quantitative Real Time-Polymerase Chain Reaction (qRT-PCR). Cell proliferation and apoptosis were measured by 3-(4, 5-dimethylthiazol-2-y1)-2, 5-diphenyl tetrazolium bromide (MTT) and flow cytometry, respectively. The levels of apoptosis-associated proteins were examined through Western blot and the concentrations of inflammatory cytokines were determined by enzyme-linked immunosorbent assay (ELISA). The targeted relationship was analyzed by Dual-Luciferase reporter assay.

RESULTS: NEAT1 was upregulated in serum of patients with atherosclerosis and HUVECs treated with ox-LDL. Knockdown of NEAT1 exerted the promotion of proliferation but suppression of apoptosis and inflammation in ox-LDL-treated HUVECs. Moreover, NEAT1 targeted miR-30c-5p and the overexpression of miR-30c-5p reversed the ox-LDL-induced effects in HUVECs. Furthermore, miR-30c-5p directly refrained the TCF7 level, and NEAT1 repression decreased the expression of TCF7 by upregulating miR-30c-5p. The knockdown of NEAT1 afforded the protective effect for HUVECs treated with ox-LDL through miR-30c-5p/TCF7 axis.

CONCLUSIONS: The knockdown of NEAT1 overtly motivated proliferation but alleviated the apoptosis and inflammation in ox-LDL-treated HUVECs by miR-30c-5p/TCF7 axis. NEAT1 accelerated the progression of atherosclerosis therapies, functioning as an indicative element.

Key Words:
NEAT1, Atherosclerosis, Inflammation, MiR-30c-5p, TCF7.

Introduction

As a frequent inflammatory disease, atherosclerosis causes the assemblage of lipids and fibrinogen in the wide arteries to form the blood plaques and stenotic arteries, bringing a series of threatening complications[1,2]. On account of the ubiquitous inflammation in every stage (commence of plaque to fracture) of atherosclerosis, inflammatory cytokines generate enormous function in the evolution of atherosclerotic injuries, such as common Interleukin-6 (IL-6), Interleukin-1β (IL-1β), and tumor necrosis factor-α (TNF-α)[3,4]. Oxidized low-density lipoprotein (ox-LDL) is a dominating risk factor of atherosclerosis and contributes to the expression of pro-inflammatory cytokines for further generating atherosclerotic plaques by acting on diverse kinds of cells, including endothelial cells, macrophages, smooth muscle cells, and stem cells[5,6]. There are increasing treatments for atherosclerosis, such as anti-inflammatory exerkines[7], sonodynamic therapy[8], drug therapy[9], and so on. But because of the dissatisfactory therapeutic efficacy, the exploration of pathological mechanism and molecular targets of atherosclerosis is pressing.

Long non-coding RNAs (lncRNAs) are a category of long, competing endogenous RNAs (ceRNAs) with more than 200 nucleotides[10]. LncRNAs were considered to regulate the cancer development due to the favorable regulatory role[11], and numerous studies manifested that growing lncRNAs were closely related to the progression of atherosclerosis[12-14], including nuclear-enriched abundant transcript (NEAT1). NEAT1, localized

Corresponding Author: Hongbo Yu, MD; e-mail: useflo@163.com

in nuclear paraspeckle, was reported to enhance the ox-LDL-induced inflammation response in macrophages *via* paraspeckle shaping[15], implying that NEAT1 might play the momentous part in the inflammation of atherosclerotic cells. By comparison with lncRNAs, microRNAs (miRNAs) are shorter with only 21-25 nucleotides[16]. But as representative post-transcriptional regulators, miRNAs also actively participate in the process of atherosclerosis. Thereinto, the low expression of miR-30c-5p was surprisingly found in atherogenesis[17]. But different from the abundant cancer researches, more exploratory studies of NEAT1 and miR-30c-5p in atherogenesis are necessary.

Transcription factor 7 (TCF7), also called T-cell-specific transcription factor-1 (TCF-1), was showed to be conducive to the advancement of multiple cancers and diseases, including nasopharyngeal carcinoma[18], colorectal cancer[19], gastric cancer[19], altered hepatic physiology during type 2 diabetes[20], and so on. Moreover, Zhu et al[21] declared that TCF7 played a crucial role in the production of inflammatory factors in lung diseases. However, there is little report of TCF7 on the inflammation in atherogenesis.

Our study was designed to investigate the molecular mechanism of NEAT1 in the process of atherogenesis. In detail, the levels and impacts of NEAT1, miR-30c-5p and TCF7 in ox-LDL-treated human umbilical vein endothelial cells (HUVECs) were measured, and their correlation was explored through further execution of experiments and analysis of data.

Patients and Methods

Serum Collection

Serum specimens were acquired from 30 patients attacked by atherosclerosis at the First Hospital of Jilin University. Atherosclerotic patients were included or excluded in line with ESC Guidelines on the diagnosis and treatment of peripheral artery diseases. Normal serum specimens were gained from 20 healthy individuals in the Physical Examination Center at this hospital. These samples were preserved at -80°C right away. All participants of this serum collection signed the written informed consents. The approval of this report was given by the Ethics Committee of the First Hospital of Jilin University.

Cell Culture and Treatment

After purchase from American Type Culture Collection (ATCC; Manassas, VA, USA), HUVECs were cultivated in F-12K medium (Gibco, Carlsbad, CA, USA) in a 37°C incubator with 95% wettish air and 5% CO_2. Specifically, the supplement of 10% fetal bovine serum (FBS; Gibco, Carlsbad, CA, USA) and antibiotics (100 U/mL penicillin and 100 μg/mL streptomycin; Gibco, Carlsbad, CA, USA) was required.

To simulate the primary stage of atherosclerosis, HUVECs were treated with ox-LDL from Beijing Xiesheng Biotechnology Co., Ltd. (Beijing, China) at different concentrations (0 μg/mL, 15 μg/mL, 30 μg/mL and 45 μg/mL). After treatment with ox-LDL for 24 h, cells were applied to the following assays.

Cell Transfection

Small interfering RNA (siRNA) against NEAT1 (si-NEAT1#1 and si-NEAT1#2), miR-30c-5p mimic (miR-30c-5p), miR-30c-5p inhibitor (anti-miR-30c-5p), pcDNA-TCF7 overexpression vector (TCF7) and respective negative controls (si-NC, miR-NC, anti-miR-NC and pcDNA) were bought from GENEWIZ (Suzhou, China). HUVECs were inoculated into a 96-well plate and cultured to 80% confluence, then, the mixtures of vectors/oligonucleotides-Lipofectamine 3000 reagent (Invitrogen, Carlsbad, CA, USA) were added to HUVECs. At the suitable time post-transfection, the cells were harvested for subsequent experiments.

Quantitative Real Time-Polymerase Chain Reaction (qRT-PCR)

According to the producers' directions, extracted RNA was reversely transcribed into complementary DNA (cDNA) using PrimeScript™ RT Master Mix Kit (TaKaRa, Dalian, China), and the qRT-PCR reaction was implemented *via* TB Green® Premix Ex Taq™ II Kit (TaKaRa, Dalian, China) with cDNA as the template. The relative expression levels were detected with glyceraldehyde-3-phosphate dehydrogenase (GAPDH) and small nuclear RNA U6 as references and calculated through the $2^{-\Delta\Delta Ct}$ approach. All primers were synthesized from GENEWIZ: NEAT1 (forward: 5'-TGGCTAGCTCAGGGCTTCAG-3', reverse: 5'-TCTCCTTGCCAAGCTTCCTTC-3'); miR-30c-5p (forward: 5'-GCCGCTGTAAACATCCTACACT-3', reverse: 5'-GTGCAGGGTCCGAGGT-3'); TCF7 (forward: 5'-CTGGGCAAGGAAGCCATAGG-3', reverse: 5'-TGCT-

GTACCTGTGTGCTCTG-3'); GAPDH (forward: 5'-ACAACTTTGGTATCGTGGAAGG-3', reverse: 5'-GCCATCACGCCACAGTTTC-3'); U6 (forward: 5'-CGGGTGCTCGCTTCGCAGC-3', reverse: 5'-CCAGTGCAGGGTCCGAGGT-3').

3-(4, 5-Dimethylthiazol-2-y1)-2, 5-Diphenyl Tetrazolium Bromide (MTT) Assay

Cell proliferation ability was daily measured through MTT at 0-3 d after transfection. HUVECs were incubated with 10 μL MTT (Invitrogen, Carlsbad, CA, USA) for 4 h, and viable cells could convert the MTT to insoluble formazan, which was solubilized through the incubation with 100 μL dimethyl sulfoxide (DMSO; Invitrogen, Carlsbad, CA, USA). Whereafter, formazan concentration was assessed by optical density (OD) value of 490 nm through the microplate reader (Thermo Fisher Scientific, Waltham, MA, USA).

Flow Cytometry

At first, HUVECs were harvested with trypsin (Gibco, Carlsbad, CA, USA) and washed by cold phosphate-buffered saline (PBS; Gibco, Carlsbad, CA, USA). Next, Alexa Fluor® 488 annexin V and propidium iodide (PI) Kit (Invitrogen, Carlsbad, CA, USA) were used to stain cells, following the operating procedure. Ultimately, stained cells were analyzed by flow cytometer (BD Bioscience, Franklin Lakes, NJ, USA).

Western Blot

After extraction of total proteins by lysis buffer (Thermo Fisher Scientific, Waltham, MA, USA), sodium dodecyl sulfate-polyacrylamide gel electrophoresis (SDS-PAGE) was administrated to separate proteins for about 90 min. Next, separated proteins were transferred onto the polyvinylidene difluoride (PVDF) membranes (Abcam, Cambridge, UK), following by the blockade using 5% skim milk (Thermo Fisher Scientific, Waltham, MA, USA) for 3 h. Then, the incubation of primary antibodies was implemented for 4 h at room temperature, and the primary antibodies were listed below: anti-B-cell lymphoma-2 (anti-Bcl-2; Abcam, Cambridge, UK, ab32124, 1:1000), anti-Bcl-2-Associated X (anti-Bax; Abcam, Cambridge, UK, ab32503, 1:1000), anti-Cleaved-caspase3 (anti-Cleaved-casp-3; Abcam, Cambridge, UK, ab32503, 1:1000), anti-TCF7 (Abcam, Cambridge, UK, ab134127, 1:1000) and anti-GAPDH (Abcam, Cambridge, UK, ab9485, 1:3000). Afterwards, the membranes were washed by 0.05% PBS with Tween 20 (PBST; Invitrogen, Carlsbad, CA, USA) and incubated using peculiar secondary antibody (Abcam, Cambridge, UK, ab205718, 1:5000) for 45 min. Finally, the emergence of protein bands was observed through enhanced chemiluminescence (ECL) reagent (Thermo Fisher Scientific, Waltham, MA, USA).

Enzyme-Linked Immunosorbent Assay (ELISA)

The concentrations of inflammatory cytokines Interleukin-6 (IL-6), Interleukin-1β (IL-1β) and tumor necrosis factor-alpha (TNF-α) were measured using ELISA kits (BD Bioscience, Franklin Lakes, NJ, USA). In brief, the 96-well plate was coated with primary antibodies anti-IL-6 (Abcam, Cambridge, UK, ab6672, 1:500), anti-IL-1β (Abcam, Cambridge, UK, ab9722, 1:500) and anti-TNF-α (Abcam, Cambridge, UK, ab6671, 1:500) at 4°C overnight. Then, the plate was washed by 0.05% PBST (Invitrogen, Carlsbad, CA, USA) and added with diluted specimens for 2 h at 37°C. Subsequently, enzyme-labeled antibody (Abcam, Cambridge, UK, ab205718, 1:1000) was added for 45 min. The relative concentrations were recorded within 30 min after addition with stop buffer.

Dual-Luciferase Reporter Assay

StarBase3.0 and TargetScan were used for predicting the targets of lncRNA and miRNA, respectively. The sequences of wide-type (WT) NEAT1 and 3'-UTR of WT-TCF7 containing the binding sites of miR-30c-5p were inserted into pGL3 vector (Promega, Madison, WI, USA) to gain Luciferase reporter plasmids of NEAT1-WT and TCF7-WT. And their mutant-type (MT) controls (NEAT1-MUT and TCF7-MUT) were constructed. Therewith, HUVECs were co-transfected with each plasmid and miR-30c-5p or miR-NC. Eventually, the detection of relative Luciferase activity was carried out with the Dual-Luciferase reporter system (Promega, Madison, WI, USA), according to the instruction manual.

Statistical Analysis

Data were processed utilizing SPSS 19.0 (IBM Corp., Armonk, NY, USA) and GraphPad Prism 7 (La Jolla, CA, USA). By experimental convention, all results were independently conducted three times and expressed as the mean ± standard deviation (SD). The linear correlation in serum samples with atherosclerosis was analyzed

through Spearman's correlation coefficient. Student's *t*-test and one-way analysis of variance (ANOVA) followed by Tukey's test were used for the difference analysis. The difference was statistically significant when $p < 0.05$.

Results

NEAT1 Was Upregulated in Serum of Patients with Atherosclerosis and HUVECs Treated with ox-LDL

To detect the expression of NEAT1 in atherosclerosis process, the serum samples were collected and HUVECs were treated with ox-LDL. As shown in Figure 1A, NEAT1 level was higher in serum with atherosclerosis than that in normal serum. With the rising of ox-LDL concentration (0 μg/mL, 15 μg/mL, 30 μg/mL, 45 μg/mL), the expression of NEAT1 was increasingly high in HUVECs (Figure 1B). The overexpression of NEAT1 in serum with atherosclerosis and ox-LDL-treated HUVECs implied the crucial role of NEAT1 in the process of atherosclerosis.

Knockdown of NEAT1 Facilitated Proliferation but Suppressed Apoptosis and Inflammation in ox-LDL-Treated HUVECs

The interference efficiencies of si-NEAT1#1 and si-NEAT1#2 were first assessed in HUVECs. A distinct reduction of NEAT1 expression was caught in both si-NEAT1#1 and si-NEAT1#2 groups (Figure 2A), and the excellent si-NEAT1#1 was used for succedent assays. With the view of exploring the function of NEAT1 in atherosclerosis, HUVECs were treated with ox-LDL (30 μg/mL) for 24 h, and then, transfected with si-NEAT1#1. MTT revealed that ox-LDL drastically reduced the proliferation of HUVECs, but si-NEAT1#1 transfection inversely obstructed this reduction (Figure 2B). Also, the increase of apoptotic rate in ox-LDL-treated HUVECs was relatively decreased after transfection with si-NEAT1#1 (Figure 2C). Contrasted to ox-LDL group, Bcl-2 (apoptosis inhibited marker) expression was enhanced (Figure 2D) but the levels of Bax and Cleaved-casp-3 (apoptosis promoted markers) were descended (Figure 2E and F) in ox-LDL+si-NEAT1#1 group. Besides, ELISA reflected that the concentrations of IL-6 (Figure 2G), IL-1β (Figure 2H), and TNF-α (Figure 2I) were lower in ox-LDL+si-NEAT1#1 group than these in ox-LDL group. Whole data demonstrated that si-NEAT1#1 weakened the ox-LDL-induced inhibition of proliferation but increased apoptosis and inflammation, insinuating that NEAT1 knockdown promoted proliferation but refrained apoptosis and inflammation in ox-LDL-treated HUVECs.

NEAT1 Targetedly Regulated MiR-30c-5p Expression

The targeted miRNA of NEAT1 was predicted using StarBase 3.0, in which NEAT1-WT contained the binding points with miR-30c-5p, and the binding points were mutated as NEAT1-MUT (Figure 3A). In Dual-Luciferase reporter assay, the relative Luciferase activity of NEAT1-WT group was lower than that of NEAT1-MUT group after miR-30c-5p was overexpressed (Figure 3B). Compared with si-NC group, an evident ascent of miR-30c-5p expression was observed in si-NEAT1#1 group (Figure 3C). Addition-

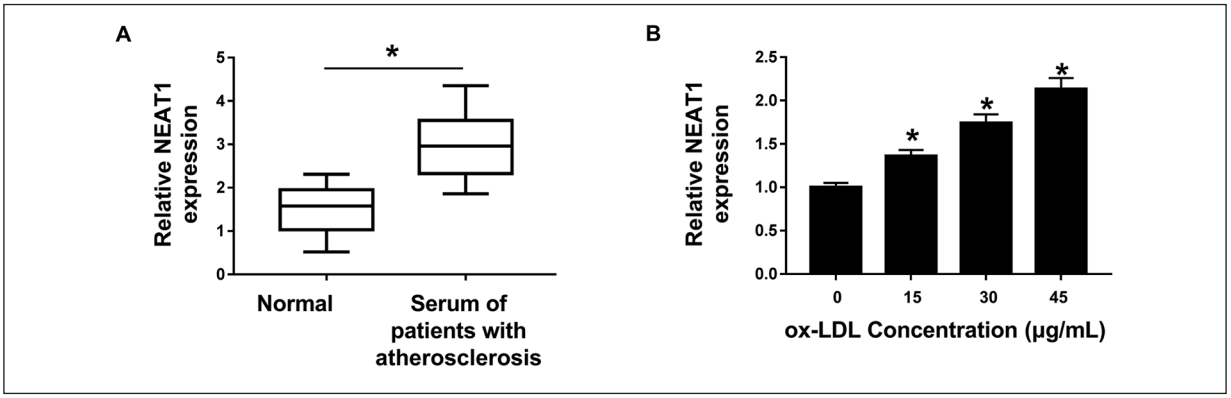

Figure 1. NEAT1 was upregulated in serum of patients with atherosclerosis and HUVECs treated with ox-LDL. **A,** and **B,** QRT-PCR was applied to examine the level of NEAT1 in serum of patients with atherosclerosis or serum of normal individuals (**A**) and HUVECs treated with ox-LDL (0 μg/mL, 15 μg/mL, 30 μg/mL, 45 μg/mL) (**B**). *$p < 0.05$.

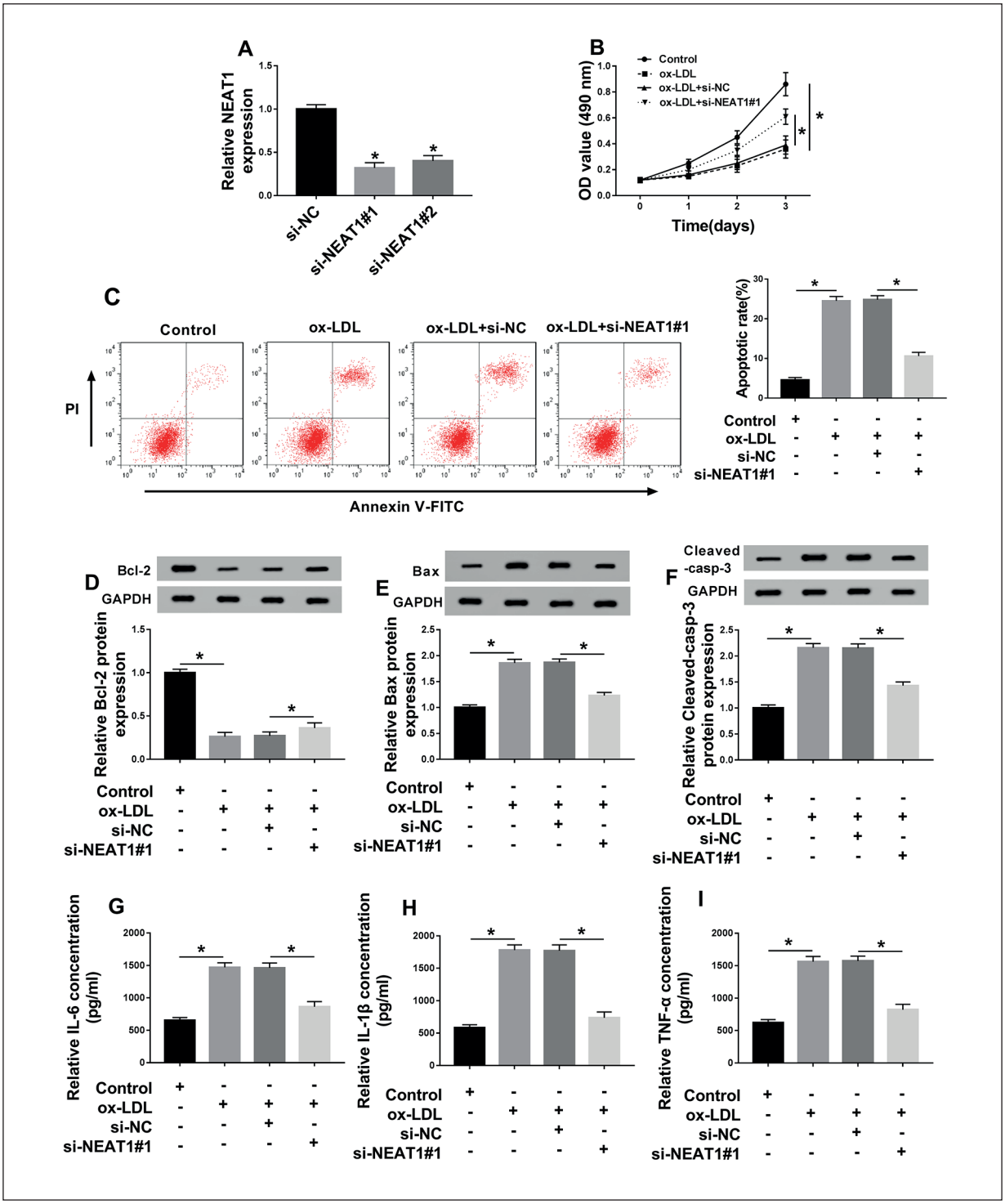

Figure 2. Knockdown of NEAT1 facilitated proliferation but suppressed apoptosis and inflammation in ox-LDL-treated HUVECs. **A,** The interference efficiencies of si-NEAT1#1 and si-NEAT1#2 were assessed by qRT-PCR. **B,** Cell proliferation was examined by MTT in HUVECs treated with ox-LDL (30 μg/mL) and transfected with si-NEAT1#1 or relative controls. **C,** Cell apoptosis was detected through flow cytometry. (D-F) Western blot was utilized for detecting the levels of Bcl-2 (**D**), Bax (**E**) and Cleaved-casp-3 (**F**). **G-I,** ELISA was used to determine the concentrations of IL-6 (**G**), IL-1β (**H**) and TNF-α (**I**). *$p < 0.05$.

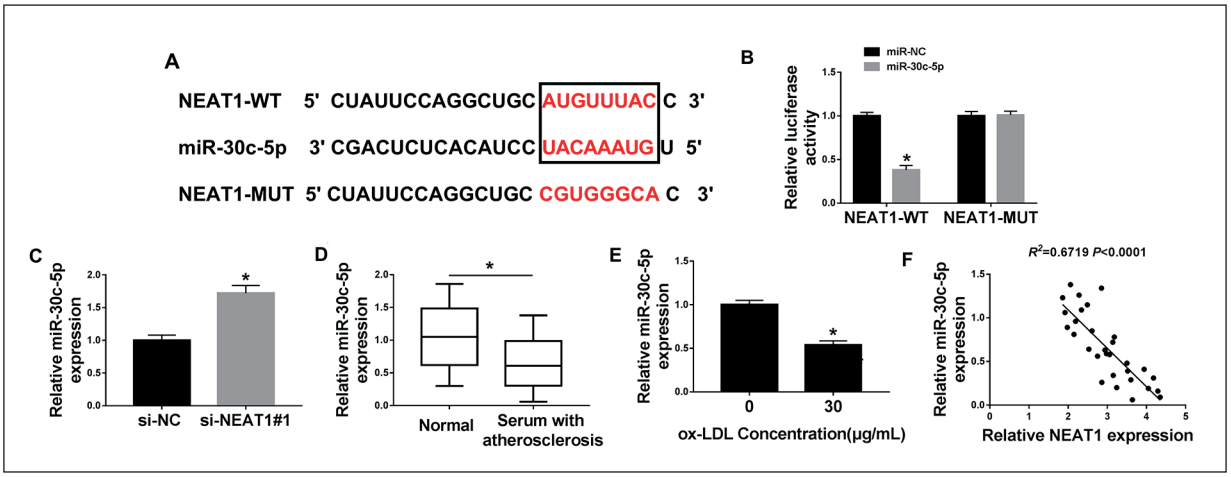

Figure 3. NEAT1 targetedly regulated miR-30c-5p expression. **A,** Presumptive binding sites between NEAT1 and miR-30c-5p were predicted by Starbase3.0. **B,** The targeted relation was evaluated by dual-luciferase reporter assay. **C,** The level of miR-30c-5p was measured in HUVECs transfected with si-NEAT1#1 or si-NC. **D,** and **E,** QRT-PCR was performed to examine miR-30c-5p expression in serum with atherosclerosis (**D**) and HUVECs treated with ox-LDL (30 μg/mL). **F,** The analysis of liner relation between NEAT1 and miR-30c-5p in serum with atherosclerosis was carried out by Spearman's correlation coefficient. *$p < 0.05$.

ally, qRT-PCR manifested that miR-30c-5p was remarkedly downregulated in serum of patients with atherosclerosis (Figure 3D) and HUVECs treated with ox-LDL (30 μg/mL) (Figure 3E) in comparison to normal serum and HUVECs without ox-LDL. We found a negative relation between NEAT1 and miR-30c-5p in serum with atherosclerosis (R^2=0.7168, p<0.0001) (Figure 3F). Above results suggested that NEAT1 directly targeted miR-30c-5p and modulated its expression.

Upregulation of MiR-30c-5p Relieved the ox-LDL-Induced Effects on Proliferation, Apoptosis and Inflammation in ox-LDL-Treated HUVECs

MiR-30c-5p was firstly transfected into HUVECs and the overexpression effect was conspicuous compared with miR-NC group (Figure 4A). After treatment with ox-LDL (30 μg/mL) for 24 h and transfection with miR-30c-5p, a series of experiments about biological behaviors were conducted to investigate the potential action of miR-30c-5p in atherosclerosis. As Figure 4B depicted, the descent of cell proliferation induced by ox-LDL was ameliorated by transfection with miR-30c-5p in HUVECs. Similarly, the ox-LDL-induced promoted effect on apoptosis was abated by elevating miR-30c-5p (Figure 4C). Meanwhile, miR-30c-5p transfection mitigated the ox-LDL-induced repression of Bcl-2 (Figure 4D) but motivation of Bax (Figure 4E) and Cleaved-casp-3 (Figure 4F) in HUVECs. Similarly, ox-LDL clearly facilitated the inflammation because of the rising of IL-6 (Figure 4G), IL-1β (Figure 4H) and TNF-α (Figure 4I), while this rising was alleviated after the overexpression of miR-30c-5p. Therefore, ox-LDL-induced effects on proliferation, apoptosis and inflammation in ox-LDL-treated HUVECs were all lightened through the promotion of miR-30c-5p.

MiR-30c-5p Directly Combined With TCF7 and Restrained the Expression of TCF7

To seek the target gene of miR-30c-5p, the matched binding sites of miR-30c-5p in the position of TCF7 3'UTR (372-379) were predicted by TargetScan (Figure 5A), and the lower Luciferase activity was detected through the co-transfection of TCF7-WT and miR-30c-5p (Figure 5B). Notably, the overexpression of miR-30c-5p refrained TCF7 mRNA (Figure 5C) and protein (Figure 5D) levels in HUVECs. In the serum of atherosclerosis patients, the mRNA (Figure 5E) and protein (Figure 5F) levels of TCF7 were significantly upregulated. Besides, the mRNA expression of TCF7 was higher (Figure 5G), as well as TCF7 protein expression (Figure 5H), in the presence of ox-LDL (30 μg/mL) than the absence of that in HUVECs. Moreover, the liner relation between miR-30c-5p and TCF7 levels in serum of patients with atherosclerosis was prominently negative (R^2=0.7089, p<0.0001) (Figure 5I). Probably, miR-30c-5p directly inhibited TCF7 expression.

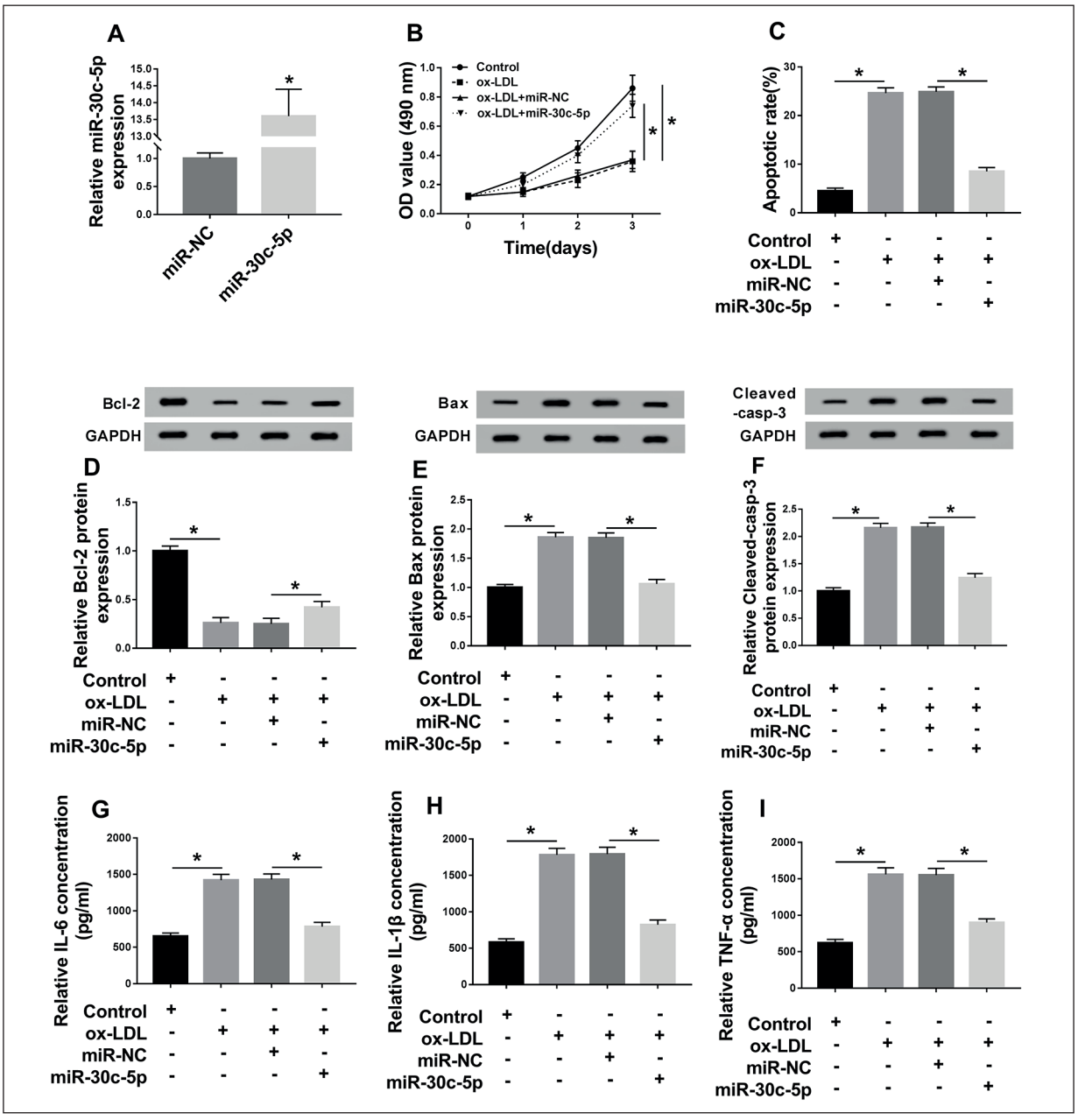

Figure 4. Upregulation of miR-30c-5p relieved the ox-LDL-induced effects on proliferation, apoptosis and inflammation in ox-LDL-treated HUVECs. **A,** The assessment of overexpression efficiency of miR-30c-5p was administrated by qRT-PCR. **B,** MTT was used for detecting the proliferation ability in ox-LDL, ox-LDL+ miR-30c-5p groups or matched controls in HUVECs. **C,** Flow cytometry was conducted to examine apoptotic cells. **D-F,** The protein levels of Bcl-2 (**D**), Bax (**E**) and Cleaved-casp-3 (**F**) were measured through Western blot. **G-I,** The concentrations of IL-6 (**G**), IL-1β (**H**) and TNF-α (**I**) were tested via ELISA. *$p < 0.05$.

Depression of NEAT1 Restrained TCF7 Expression Via Enhancing MiR-30c-5p

After the analysis between the expression of NEAT1 and TCF7 in serum of patients with atherosclerosis, a positive correlation (R^2=0.6664, p<0.0001) was discovered (Figure 6A). Whereafter, HUVECs were transfected with six groups (si-NC, si-NEAT1#1, si-NEAT1#1+anti-miR-NC, si-NEAT1#1+anti-miR-30c-5p, miR-30c-5p+pcDNA, miR-30c-5p+TCF7), and then, TCF7 expression was measured using QRT-PCR and Western blot. As presented in Figure 6B and C, transfection with si-NEAT1 decreased both mRNA and protein expression of TCF7, but miR-30c-5p inhibitor reverted these decreased effects. MiR-30c-5p-induced repression of TCF7 mRNA and protein levels were

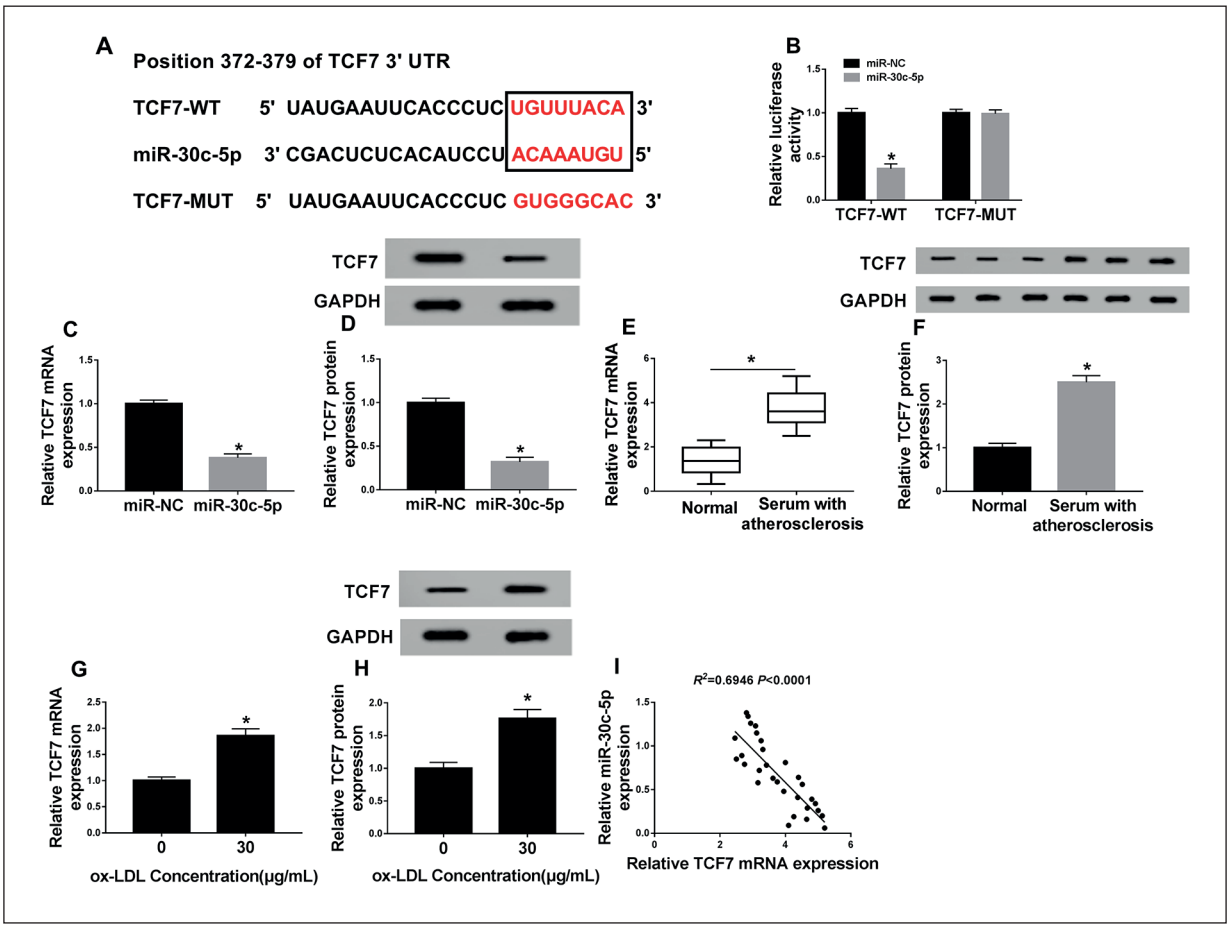

Figure 5. MiR-30c-5p directly combined with TCF7 and restrained the expression of TCF7. **A,** TargetScan was used for analyzing the combination between miR-30c-5p and TCF7. **B,** Dual-Luciferase reporter assay was executed for the luciferase activity in HUVECs co-transfected with TCF7-WT or TCF7-MUT and miR-30c-5p or miR-NC. **C,** and **D,** TCF7 mRNA and protein levels in HUVECs transfected with miR-30c-5p or miR-NC were examined through QRT-PCR and Western blot. **E-H,** QRT-PCR and Western blot were implemented for determining the mRNA and protein levels of TCF7 in serum with atherosclerosis (E and F) and HUVECs treated with ox-LDL (30 μg/mL) (**G** and **H**). **I,** Spearman's correlation coefficient was used for analyzing the liner relation between miR-30c-5p and TCF7 in serum with atherosclerosis. *$p < 0.05$.

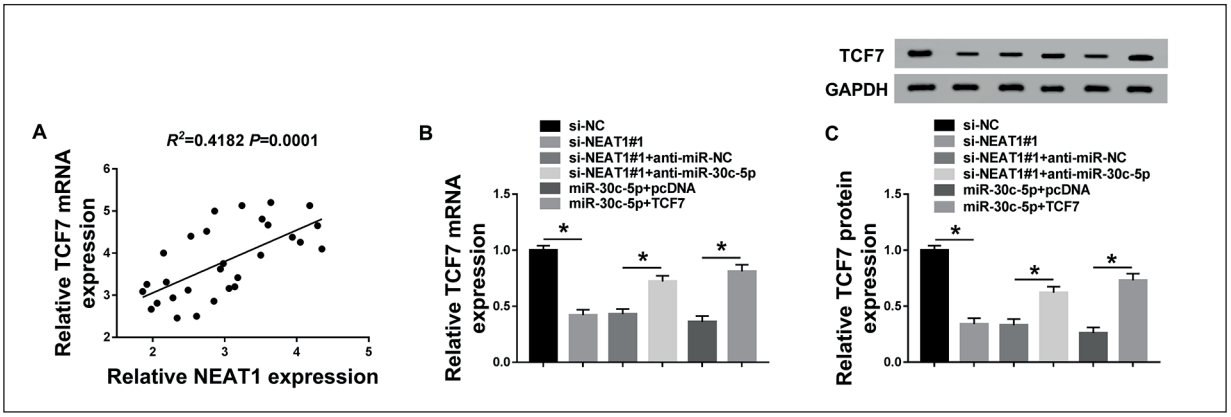

Figure 6. Depression of NEAT1 restrained TCF7 expression via enhancing miR-30c-5p. **A,** The relationship between NEAT1 and TCF7 in serum of patients with atherosclerosis was evaluated by Spearman's correlation coefficient. **B,** and **C,** The analysis of TCF7 mRNA and protein expression was administrated utilizing QRT-PCR and Western blot after transfection with si-NC, si-NEAT1#1, si-NEAT1#1+anti-miR-NC, si-NEAT1#1+anti-miR-30c-5p, miR-30c-5p+pcDNA, miR-30c-5p+TCF7. *$p < 0.05$.

abrogated by TCF7 overexpression. These results testified that the reduction of NEAT1 had a suppressive effect on TCF7 expression by motivating the level of miR-30c-5p.

Downregulation of NEAT1 Provided the Protective Effect for ox-LDL-Treated HUVECs by MiR-30c-5p/TCF7 Axis

To analyze the regulatory mechanism of NEAT1 in atherosclerosis process, HUVECs were treated with ox-LDL (30 μg/mL) for 24 h and transfected with six groups as Figure 6. Firstly, MTT revealed that anti-miR-30c-5p transfection memorably declined the OD value protected by si-NEAT1#1, and overexpression of TCF7 reverted the promoted effect on OD value induced by miR-30c-5p (Figure 7A). Then, miR-30c-5p inhibitor expedited apoptosis decreased by si-NEAT1#1, and transfection of TCF7 promoted the miR-30c-5p-reduced cell apoptosis (Figure 7B). Simultaneously, Bcl-2 expression was elevated by si-NEAT1#1 but was suppressed after transfection with anti-miR-30c-5p, and the level of Bcl-2 was lower in miR-30c-5p+TCF7 group than that in miR-30c-5p+pcDNA

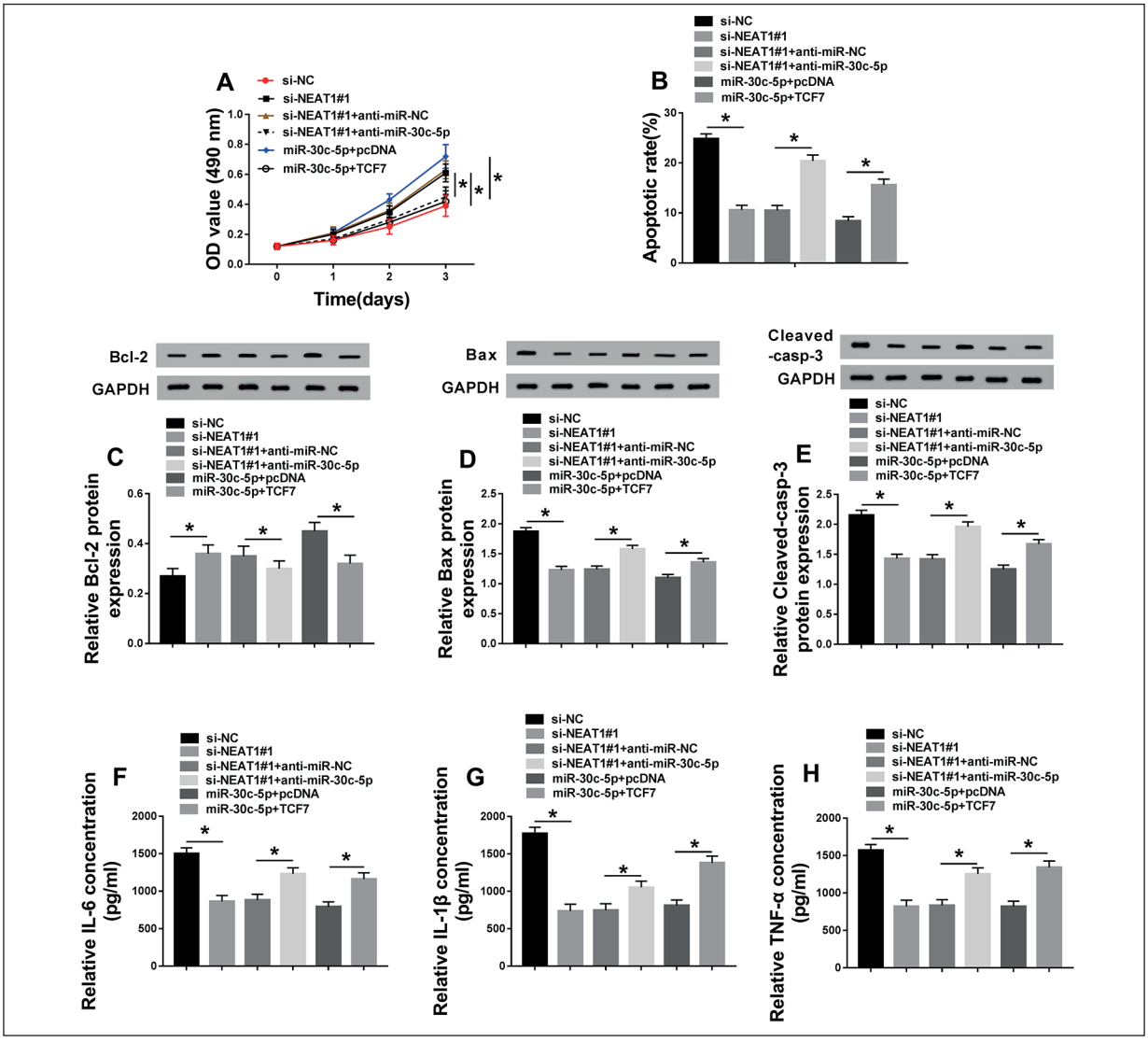

Figure 7. Downregulation of NEAT1 provided the protective effect for ox-LDL-treated HUVECs by miR-30c-5p/TCF7 axis. **A,** The detection of cell proliferation was conducted by MTT in HUVECs treated with ox-LDL (30 μg/mL) and transfected with si-NC, si-NEAT1#1, si-NEAT1#1+anti-miR-NC, si-NEAT1#1+anti-miR-30c-5p, miR-30c-5p+pcDNA, miR-30c-5p+TCF7. **B,** Examination of apoptosis was implemented by flow cytometry. **C-E,** The assessment of Bcl-2 (**C**), Bax (**D**) and Cleaved-casp-3 (**E**) levels was conducted using Western blot. **F-H,** The testing of the concentrations of IL-6 (**F**), IL-1β (**G**) and TNF-α (**H**) was executed through ELISA. *$p < 0.05$.

group (Figure 7C). Also, the lessening of both Bcl-2 (Figure 7D) and cleaved-casp-3 (Figure 7E) caused by si-NEAT1#1 or miR-30c-5p was enhanced by adding anti-miR-30c-5p or TCF7, respectively. Moreover, miR-30c-5p inhibitor markedly reversed the inhibitory effects of si-NEAT1#1 on IL-6 (Figure 7F), IL-1β (Figure 7G) and TNF-α (Figure 7H), and the miR-30c-5p-induced effects were abolished by promoting TCF7. Collectively, the knockdown of NEAT1 motivated proliferation but decreased apoptosis and inflammation induced by ox-LDL by inhibiting TCF7 and by heightening miR-30c-5p, exerting the protective effect for the HUVECs treated with ox-LDL and contributing to relieve the injury of atherosclerosis.

Discussion

Atherosclerosis is largely responsible for the occurrence of thrombosis, myocardial infarction, stroke, and coronary heart disease[2,22], which causes aggressive damage for public health. In consideration of the complicacy of atherosclerosis pathology and multitudinous complications, the emergence of novel targets might be a breakthrough to meet the current change of unsatisfactory effect. During our report, we had a thorough knowledge of the role of NEAT1 in atherosclerosis and disclosed the receivable mechanism. NEAT1 was upregulated in serum of patients with atherosclerosis and ox-LDL-treated HUVECs, and knockdown of NEAT1 could elevate proliferation but weaken apoptosis and inflammation in HUVECs treated with ox-LDL *via* regulating miR-30c-5p/TCF7 axis. NEAT1 is an available candidate for therapeutic targets in the treatment strategies for atherosclerosis.

Certainly, segmental reports about NEAT1 have put the highlight on the initiation and evolution of atherosclerosis and atherosclerosis-triggered diseases. For example, NEAT1 was certified to involve in some chemokines and interleukins, regulating the action of immunocyte and inhibiting the inception of myocardial infarction in patients[23]. Ma et al[24] declared that NEAT1 exacerbated the myocardial ischemia reperfusion injury in diabetic rats by inducing apoptosis and autophagy of cardiomyocyte. Gast et al[25] recorded the potential relevance between NEAT1 and immune system-mediated atherosclerosis. In the present study, we firstly ascertained the upregulation of NEAT1 in serum derived from patients with atherosclerosis. By reason of the indicative role of ox-LDL in atherosclerosis[26], we established the model of atherosclerosis onset *in vitro* through the treatment with ox-LDL for HUVECs. Consistent with the previous reports of the elevation of NEAT1 induced by ox-LDL[27,28], the enhancement of NEAT1 expression after treatment with ox-LDL at different concentrations was also found in this research. Preliminary results demonstrated there was an underlying positive regulation between NEAT1 expression and atherosclerosis process. To explore the precise function of NEAT1 in atherosclerosis, the significant behaviors of inflammation and apoptosis, along with cell proliferation, were measured in HUVECs treated ox-LDL (30 μg/mL). The results manifested that the decrease of cell proliferation but the increase of apoptosis and inflammation induced by ox-LDL were all rescued by NEAT1 inhibition, insinuating that the knockdown of NEAT1 had a promotion of proliferation but a reduction of apoptosis and inflammation in ox-LDL-treated HUVECs, in accord with the findings in macrophages RAW264.7[27] and THP-1[28]. The anti-apoptotic/inflammatory role of NEAT1 knockdown on atherosclerosis was exposed, suggesting that NEAT1 might be a positive indicator of atherosclerosis.

Researches of miRNAs on atherosclerosis are increasing over the few decades. Xue et al[29] alleged that miR-19b/221/222 regulated the apoptosis and inflammation of endothelial cells by inhibiting proliferator-activated receptor γ coactivator 1α (PGC-1α) in atherosclerosis process. Tang et al[30] found that miR-126 could ameliorate the injury of endothelial cells in atherosclerosis *via* recovering autophagy. Notably, miR-24[31] and miR-140-5p[32] aggravated atherosclerosis by regulating gene expression. The roles of diverse miRNAs are different in atherosclerosis. NEAT1 has been elucidated to serve as ceRNA of different miRNAs in many diseases, including atherosclerosis[27,33,34]. Taking this into consideration, we speculated that NEAT1 was relevant to certain miRNA in the progression of atherosclerosis. As expected, NEAT1 targeted miR-30c-5p and negatively regulated the expression of miR-30c-5p in HUVECs. Through the attestation of anterior studies, there was a downregulation of miR-30-5p in atherosclerosis patients and endothelial cells treated with ox-LDL[33], and miR-30c-5p alleviated atherosclerosis *via* inhibiting endothelial cell pyroptosis[34] and macrophage-mediated inflammation[35]. In line with

these findings, our study indicated that miR-30c-5p was downregulated in serum of patients with atherosclerosis and ox-LDL-treated HUVECs, and miR-30c-5p reversed the ox-LDL-induced inhibition of proliferation but the acceleration of apoptosis and inflammation in ox-LDL-treated HUVECs, notarizing the anti-atherosclerosis role of miR-30c-5p.

Due to the character of miRNAs by regulating the expression of downstream genes, an interesting assumption was appeared that NEAT1 might function as a miR-30c-5p sponge *via* regulating gene expression. In this research, TCF7 was deemed as a presumptive target of miR-30c-5p by TargetScan prediction, and the negatively targeted relation between miR-30c-5p and TCF7 was further validated. Moreover, TCF7 level was heightened not only in serum of patients with atherosclerosis but also in ox-LDL-treated HUVECs, in consistent with the elevation of TCF7 in the process of atherosclerosis as previously reported[36-38]. Subsequently, we found a positive correlation between NEAT1 and TCF7 expression, and the knockdown of NEAT1 could reduce the expression of TCF7 through the motivation of miR-30c-5p. Furthermore, NEAT1 knockdown had the protective function for HUVECs treated with ox-LDL via miR-30c-5p/TCF7 axis, confirming the NEAT1/miR-30c-5p/TCF7 regulatory axis in the progression of atherosclerosis.

Conclusions

To summarize, there was a detailed elucidation on the role and modulatory mechanism of NEAT1 in atherosclerosis in our report. The knockdown of NEAT1 could facilitate proliferation but repress apoptosis and inflammation in HUVECs treated with ox-LDL *via* downregulating TCF7 by promoting miR-30c-5p. Innovatively, we expounded a new regulatory mechanism of NEAT1/miR-30c-5p/TCF7 axis in atherosclerosis, which might break the restriction of traditional therapies and exploit an upgraded perspective with NEAT1 as a therapeutic target for confronting atherosclerosis. Hence, the prospect of atherosclerosis is gradually bright in the direct clinical treatments partly through the regulatory mechanism of NEAT1.

Conflict of Interest

The Authors declare that they have no conflict of interests.

References

1) Libby P, Ridker PM, Maseri A. Inflammation and atherosclerosis. Circulation 2002; 105: 1135-1143.
2) Lusis AJ. Atherosclerosis. Nature 2000; 407: 233-241.
3) Khan R, Spagnoli V, Tardif JC, L'Allier PL. Novel anti-inflammatory therapies for the treatment of atherosclerosis. Atherosclerosis 2015; 240: 497-509.
4) Kirichenko TV, Sobenin IA, Nikolic D, Rizzo M, Orekhov AN. Anti-cytokine therapy for prevention of atherosclerosis. Phytomedicine 2016; 23: 1198-1210.
5) Yang H, Mohamed AS, Zhou SH. Oxidized low density lipoprotein, stem cells, and atherosclerosis. Lipids Health Dis 2012; 11: 85.
6) Kattoor AJ, Kanuri SH, Mehta JL. Role of Ox-LDL and LOX-1 in atherogenesis. Curr Med Chem 2019; 26: 1693-1700.
7) Yu M, Tsai SF, Kuo YM. The therapeutic potential of anti-inflammatory exerkines in the treatment of atherosclerosis. Int J Mol Sci 2017; 18: pii: E1260.
8) Geng C, Zhang Y, Hidru TH, Zhi L, Tao M, Zou L, Chen C, Li H, Liu Y. Sonodynamic therapy: A potential treatment for atherosclerosis. Life Sci 2018; 207: 304-313.
9) Yang Q, Wang C, Jin Y, Ma X, Xie T, Wang J, Liu K, Sun H. Disocin prevents postmenopausal atherosclerosis in ovariectomized LDLR-/- mice through a PGC-1alpha/ERalpha pathway leading to promotion of autophagy and inhibition of oxidative stress, inflammation and apoptosis. Pharmacol Res 2019; 148: 104414.
10) Ponting CP, Oliver PL, Reik W. Evolution and functions of long noncoding RNAs. Cell 2009; 136: 629-641.
11) Li CH, Chen Y. Insight into the role of long noncoding RNA in cancer development and progression. Int Rev Cell Mol Biol 2016; 326: 33-65.
12) Zhou T, Ding JW, Wang XA, Zheng XX. Long noncoding RNAs and atherosclerosis. Atherosclerosis 2016; 248: 51-61.
13) Jian L, Jian D, Chen Q, Zhang L. Long noncoding RNAs in atherosclerosis. J Atheroscler Thromb 2016; 23: 376-384.
14) Li H, Zhu H, Ge J. Long noncoding RNA: recent updates in atherosclerosis. Int J Biol Sci 2016; 12: 898-910.
15) Huang-Fu N, Cheng JS, Wang Y, Li ZW, Wang SH. Neat1 regulates oxidized low-density lipoprotein-induced inflammation and lipid uptake in macrophages via paraspeckle formation. Mol Med Rep 2018; 17: 3092-3098.
16) Cho WC. OncomiRs: the discovery and progress of microRNAs in cancers. Mol Cancer 2007; 6: 60.
17) Vilahur G. Relevance of low miR-30c-5p levels in atherogenesis: a promising predictive biomarker and potential therapeutic target. Cardiovasc Res 2017; 113: 1536-1537.
18) Zhan Y, Feng J, Lu J, Xu L, Wang W, Fan S. Expression of LEF1 and TCF1 (TCF7) proteins associ-

ates with clinical progression of nasopharyngeal carcinoma. J Clin Pathol 2019; 72: 425-430.

19) Wu B, Chen M, Gao M, Cong Y, Jiang L, Wei J, Huang J. Down-regulation of lncTCF7 inhibits cell migration and invasion in colorectal cancer via inhibiting TCF7 expression. Hum Cell 2019; 32: 31-40.

20) Kaur K, Vig S, Srivastava R, Mishra A, Singh VP, Srivastava AK, Datta M. Elevated hepatic miR-22-3p expression impairs gluconeogenesis by silencing the Wnt-responsive transcription factor Tcf7. Diabetes 2015; 64: 3659-3669.

21) Zhu Y, Wang W, Wang X. Roles of transcriptional factor 7 in production of inflammatory factors for lung diseases. J Transl Med 2015; 13: 273.

22) Pothineni NVK, Subramany S, Kuriakose K, Shirazi LF, Romeo F, Shah PK, Mehta JL. Infections, atherosclerosis, and coronary heart disease. Eur Heart J 2017; 38: 3195-3201.

23) Gast M, Rauch B, Haghikia A, Nakagawa S, Haas J, Stroux A, Schmidt D, Schumann P, Weiss S, Jensen L, Kratzer A, Kraenkel N, Muller C, Bornigen D, Hirose T, Blankenberg S, Escher F, Kuhl A, Kuss A, Meder B, Landmesser U, Zeller T, Poller W. Long noncoding RNA NEAT1 modulates immune cell functions and is suppressed in early onset myocardial infarction patients. Cardiovasc Res 2019; 115: 1886-1906.

24) Ma M, Hui J, Zhang QY, Zhu Y, He Y, Liu XJ. Long non-coding RNA nuclear-enriched abundant transcript 1 inhibition blunts myocardial ischemia reperfusion injury via autophagic flux arrest and apoptosis in streptozotocin-induced diabetic rats. Atherosclerosis 2018; 277: 113-122.

25) Gast M, Rauch BH, Nakagawa S, Haghikia A, Jasina A, Haas J, Nath N, Jensen L, Stroux A, Bohm A, Friebel J, Rauch U, Skurk C, Blankenberg S, Zeller T, Prasanth KV, Meder B, Kuss A, Landmesser U, Poller W. Immune system-mediated atherosclerosis caused by deficiency of long non-coding RNA MALAT1 in ApoE-/-mice. Cardiovasc Res 2019; 115: 302-314.

26) Hartley A, Haskard D, Khamis R. Oxidized LDL and anti-oxidized LDL antibodies in atherosclerosis - Novel insights and future directions in diagnosis and therapy. Trends Cardiovasc Med 2019; 29: 22-26.

27) Chen DD, Hui LL, Zhang XC, Chang Q. NEAT1 contributes to ox-LDL-induced inflammation and oxidative stress in macrophages through inhibiting miR-128. J Cell Biochem 2018 Sep 11. doi: 10.1002/jcb.27541. [Epub ahead of print].

28) Wang L, Xia JW, Ke ZP, Zhang BH. Blockade of NEAT1 represses inflammation response and lipid uptake via modulating miR-342-3p in human macrophages THP-1 cells. J Cell Physiol 2019; 234: 5319-5326.

29) Xue Y, Wei Z, Ding H, Wang Q, Zhou Z, Zheng S, Zhang Y, Hou D, Liu Y, Zen K, Zhang CY, Li J, Wang D, Jiang X. MicroRNA-19b/221/222 induces endothelial cell dysfunction via suppression of PGC-1alpha in the progression of atherosclerosis. Atherosclerosis 2015; 241: 671-681.

30) Tang F, Yang TL. MicroRNA-126 alleviates endothelial cells injury in atherosclerosis by restoring autophagic flux via inhibiting of PI3K/Akt/mTOR pathway. Biochem Biophys Res Commun 2018; 495: 1482-1489.

31) Ren K, Zhu X, Zheng Z, Mo ZC, Peng XS, Zeng YZ, Ou HX, Zhang QH, Qi HZ, Zhao GJ, Yi GH. MicroRNA-24 aggravates atherosclerosis by inhibiting selective lipid uptake from HDL cholesterol via the post-transcriptional repression of scavenger receptor class B type I. Atherosclerosis 2018; 270: 57-67.

32) Liu QQ, Ren K, Liu SH, Li WM, Huang CJ, Yang XH. MicroRNA-140-5p aggravates hypertension and oxidative stress of atherosclerosis via targeting Nrf2 and Sirt2. Int J Mol Med 2019; 43: 839-849.

33) Klec C, Prinz F, Pichler M. Involvement of the long noncoding RNA NEAT1 in carcinogenesis. Mol Oncol 2019; 13: 46-60.

34) Zhou H, Wang B, Yang YX, Jia QJ, Zhang A, Qi ZW, Zhang JP. Long Noncoding RNAs in pathological cardiac remodeling: a review of the update literature. Biomed Res Int 2019; 2019: 7159592.

35) Zhou Z, Chen Y, Zhang D, Wu S, Liu T, Cai G, Qin S. MicroRNA-30-3p suppresses inflammatory factor-induced endothelial cell injury by targeting TCF21. Mediators Inflamm 2019; 2019: 1342190.

36) Li P, Zhong X, Li J, Liu H, Ma X, He R, Zhao Y. MicroRNA-30c-5p inhibits NLRP3 inflammasome-mediated endothelial cell pyroptosis through FOXO3 down-regulation in atherosclerosis. Biochem Biophys Res Commun 2018; 503: 2833-2840.

37) Ceolotto G, Giannella A, Albiero M, Kuppusamy M, Radu C, Simioni P, Garlaschelli K, Baragetti A, Catapano AL, Iori E, Fadini GP, Avogaro A, Vigili de Kreutzenberg S. MiR-30c-5p regulates macrophage-mediated inflammation and pro-atherosclerosis pathways. Cardiovasc Res 2017; 113: 1627-1638.

38) Hartmann P, Zhou Z, Natarelli L, Wei Y, Nazari-Jahantigh M, Zhu M, Grommes J, Steffens S, Weber C, Schober A. Endothelial dicer promotes atherosclerosis and vascular inflammation by miRNA-103-mediated suppression of KLF4. Nat Commun 2016; 7: 10521.